

COMPARISON OF EXPERIMENTAL AND ANALYTICAL SOLUTIONS OF TEMPERATURE FIELD IN A SUBMERGED ARC WELDING

Antun Barac, Marija Živić, Mario Holik, Ružica Končić, Ivan Samardžić

Key words: analytical solution, temperature field, thermographic camera

Abstract:

Temperature field is of crucial importance for the understanding of heat effects on welding and weld defects. The temperature distribution determines the microstructure in the heat-affected zone as well as residual stresses and distortions of the welding construction. An infrared camera provides a two-dimensional image of the infrared emission, at the surface of the sample, from which isothermal lines and the temperature distribution can be captured. Comparison of analytical and experimental solution of temperature field in metal thin-walled sheet around the moving heat source is presented in the paper. In the experiment, temperature field is recorded using thermographic camera Vario Cam 640 Hi Res in a way that camera was moving together with a heat source so the temperature field is regarded as 2D quasi-steady. Analytical solutions for the moving line source on the thin-walled sheet and moving point source on the flat layer are computed using software Engineering Equation Solver. The isotherms from the thermograms and analytical solutions are shown in 2D diagrams and compared. It is concluded that the infrared thermography can be practical weld-monitoring option able to provide a reliable estimation.

1 INTRODUCTION

The temperature field in the welding process is very inhomogeneous and unsteady. The temperature of the material inside the weld bead varies from room temperature to the melting temperature. During the welding process, inside the weld pool, filler metals and base metals melt, solidify and recrystallize. In the heat-affected-zone, microstructural transformations occur. The temperature distribution determines the residual stresses and distortions of the welding construction as well as the changes in the microstructure. For steels, for example, the time for the cooling from 800 °C to 500 °C, the so-called $t_{8/5}$ -time, has a crucial influence on the microstructure as well as mechanical properties. Therefore, the temperature field is fundamental for the understanding and analyzing of heat effects on welding and weld defects [1].

In the middle of last century, analyses of heat transfer in the welding process were made by Rosenthal [2] and Rykalin et al. [3], who have studied classical solutions of the heat conduction

equations. They developed analytical solutions for calculation of regularly temperature field with moving heat sources. These analytical solutions have certain limitations: (1) geometry and heat input models are simplified; (2) material property values are assumed to be temperature independent; and (3) heat transfer and heat radiation from the surface to the ambient environment are often simplified or even neglected, [4]. Van Elsen et al. [5] derived the analytical solution for a uniform heat source from the solution of an instantaneous point heat source. Their results demonstrated that analytical and numerical solutions can be effectively used to calculate the temperature distribution in a semi-infinite medium for finite 3D heat sources.

This paper presents the results of the application of infrared thermography in submerged arc welding. The experimentally obtained surface temperature distribution is compared with the analytical solutions for the moving line source on the thin-walled sheet and moving point source on the flat layer which are computed using software Engineering Equation Solver.

2 MEASUREMENT SYSTEM AND EXPERIMENTAL SET-UP

Infrared system which used to measure the surface temperature of the probe was JENOPTIK VarioCAM 640 Hi Res (shown in Figure 1) with a detector Microbolometer Focal Plane Array, uncooled, with resolution 640x480 pixels. The Spectral range is 7.5...14 μm . It works with an image frequency of 60 Hz in full resolution. The thermal sensitivity is 0.05 K at 30 °C. The IR-camera is equipped with a standard lens, 1.0/30 mm, (30 x 23)°. Temperature measurement range of the camera is - 40...2000 °C and measurement accuracy ± 1.5 K (0 - 100) °C; ± 2 % (< 0 resp. > 100) °C.

The temperature field is recorded in such a way that the thermographic camera moves along with a heat source (arc). This means that the recorded temperature field is observed in the moving coordinate system, with the origin in which the heat source and thermographic camera are placed. To protect thermographic camera from possible adverse effects of high temperature, the moving heat source moves on the plate, while the thermographic camera, placed vertically under the moving source, 52 cm under the plate, moves at the same speed as the heat source moves. Figure 1. shows the experimental setup, with the infrared system.



Figure 1. *Experimental set up, with the infrared system during the welding process*

3 CALIBRATION AND DETERMINATION OF THE EMISSIVITY

The preparation and realization of experiments using the thermography systems play an important role to ensure that the measured results achieve good quality. The calibration of the infrared system is based on the concept of the black body principle. It is advisable to check the infrared system regularly. Therefore control measurements were regularly carried out using a black body source Omega BB703 (shown in Figure 3) with a temperature range of 10 to 400 °C and an accuracy of ± 1.4 °C. The aperture dimension is 29 mm. It reaches an emissivity of 0.97 and the sensor is a platinum RTD thermocouple.



Figure 2. *Thermographic camera JENOPTIK VarioCAM hr research*



Figure 3. *Black body Omega BB703*

The determination of the temperature requires the knowledge of the reliable value of the emissivity. For the metals it is important to assure high emissivity to reduce the measuring error. By oxidizing the sample plates before welding, a uniform and relatively high emissivity of the surface was achieved. The emissivity of the oxidized welding plate was measured in workshop at room temperature. A thermocouple of the reference thermometer was fixed at the surface of the probe to watch and record its temperature. By comparing the temperature of the thermocouple and the shown infrared temperature, the emissivity of the surface temperature was determined. The rough, oxidized steel plate of carbon steel W.Nr.1.0038 and with the following dimensions: 1030 mm x 530 mm x 10 mm was welded in the submerged arc welding. The emissivity of the welding plate was 0.95.

4 RESULTS

The application of the method is made for submerged arc welding (Figure 4). The molten weld and the arc zone are protected from atmospheric contamination by being “submerged” under a blanket of granular fusible flux consisting of lime, silica, manganese oxide, calcium fluoride, and other compounds. When molten, the flux becomes conductive and provides a current path between the electrode and the work. This thick layer of flux completely covers the molten metal thus preventing spatter and sparks as well as suppressing the intense ultraviolet radiation.

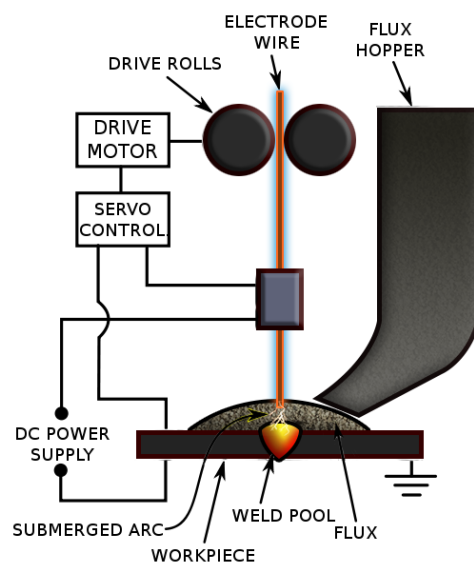


Figure 4. Experimental set up, with the infrared system during the welding process

In the following table the parameters of the welding process are given:

Table 1. Welding parameters

<i>Welding parameters</i>	
Welding machine	Welding machine KNA 1-45
Welding process	Submerged arc welding
Welding current	300 A
Welding voltage	30 V
Welding velocity	12.96 mm/s
Weld (bead) length	82 mm
Weld (bead) width	15 mm

The temperature field is measured by means of an infrared (IR) thermography system. In the experiment, the IR-camera was placed and moved together with the welding torch, and a frequency of images was 25 Hz. Thus, the quasi-steady temperature distribution is achieved which can be seen from Figures 5 and 6. They show temperature field in the 30th and 40th second of the welding process.

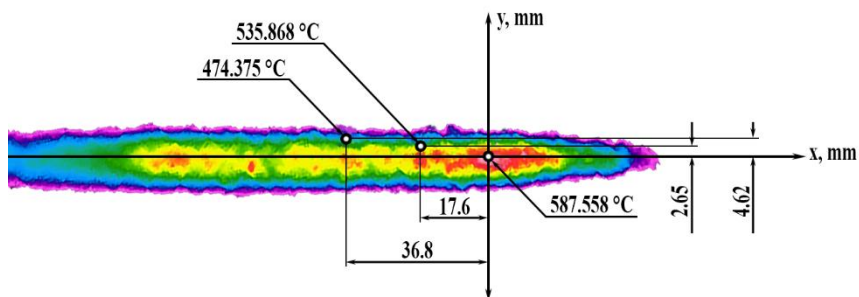


Figure 5. Temperature field in the 30th second of the welding process and coordinate system

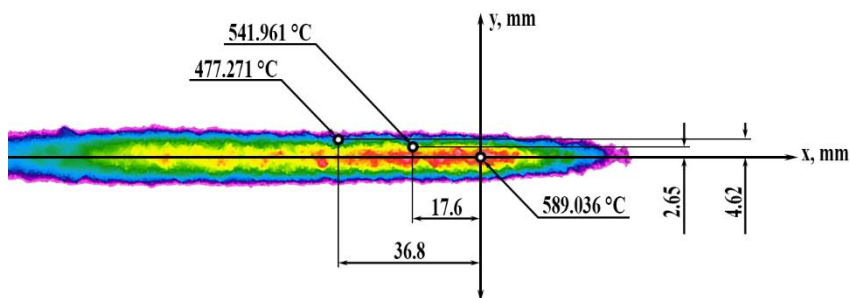


Figure 6. Temperature field in the 40th second of the welding process and coordinate system

Figures 5 and 6 show examples of infrared images with analysis spots. The values of measured temperatures will be compared with the results obtained by the calculation. Due to the stochasticity of the temperature field results, there are certain errors when reading the results. To reduce the reading error, it's necessary to calculate the mean temperature in the region of interest.

The models used for the calculation are two-dimensional (2D) quasi-steady and two and half-dimensional (2.5D) quasi-steady. These two models were compared with experimental data obtained from the thermographic camera, and a conclusion was reached on their application. 2D model could be used if results show that 10 mm thickness of the plate is enough small that the temperature on both sides is equal. In another case, 2.5D model should be considered. The temperature field can be regarded as steady-state compared to the coordinate system whose origin coincides with the position of the moving heat source on top of the plate and the position of thermographic camera on the bottom side of the plate. Temperature field is considered in both, 2D and 2.5D, models using spatial coordinates; the coordinate x , which corresponds to the direction of motion of the heat source, the perpendicular coordinate y and vertical (depth) coordinate z .

The equations for quasi-steady temperature fields, according [2] are

$$\vartheta(x, y) = \frac{\Phi}{2 \cdot \pi \cdot \lambda \cdot \delta} \cdot e^{\left(\frac{w \cdot x}{2 \cdot a}\right)} \cdot K_0 \left(r \sqrt{\frac{w^2}{4 \cdot a^2} + \frac{b}{a}} \right) \quad (1)$$

$$T(r, x, t) - T_0 = m(r, z) \cdot \frac{\Phi}{2 \cdot \pi \cdot \lambda \cdot \delta} \cdot e^{\left(\frac{w \cdot x}{2 \cdot a}\right)} \cdot K_0 \left(\frac{w \cdot r}{2 \cdot a} \right) \quad (2)$$

$$m(r, z) = 1 + \frac{2}{K_0 \left(\frac{w \cdot r}{2 \cdot a} \right)} \cdot \sum_{n=1}^{\infty} \left(\cos \left(\frac{\pi \cdot n \cdot z}{\delta} \right) \cdot K_0 \left(\frac{\pi \cdot n \cdot r}{\delta} \right) \sqrt{1 + \left(\frac{w \cdot \delta}{2 \cdot a \cdot \pi \cdot n} \right)^2} \right) \quad (3)$$

where is:

Φ - heat rate of the moving heat source

λ - thermal conductivity of the plate,

δ - plate thickness,

w - welding speed,

a - thermal diffusivity of the plate

$r = \sqrt{x^2 + y^2}$ or $\sqrt{x^2 + y^2 + z^2}$ - distance from the heat source,

$b = 2\alpha / (c\rho\delta)$, coefficient of temperature drop at the point

K_0 - operator - Bessel function of second kind and zero order

In the above equation, the following values are included to obtain the temperature field around moving heat source:

$$\begin{aligned}\Phi &= 6300 \text{ W} \\ \lambda &= 25 \text{ W/(mK)} \\ \delta &= 0.010 \text{ m,} \\ w &= 0.01296 \text{ m/s} \\ a &= 7.058 \cdot 10^{-6} \text{ m}^2/\text{s} \\ b &= 4 \cdot 10^{-3} \text{ s}^{-1}\end{aligned}$$

It's clear that the temperature field is the product of the constants and the values of the exponential and Bessel function. In the point $x = 0, y = 0$, i.e. in the point where heat source is fixed, value of the temperature tends to infinity because $K_0(0) \rightarrow \infty$. This means that in the immediate environment around the heat source very large temperature gradients appear.

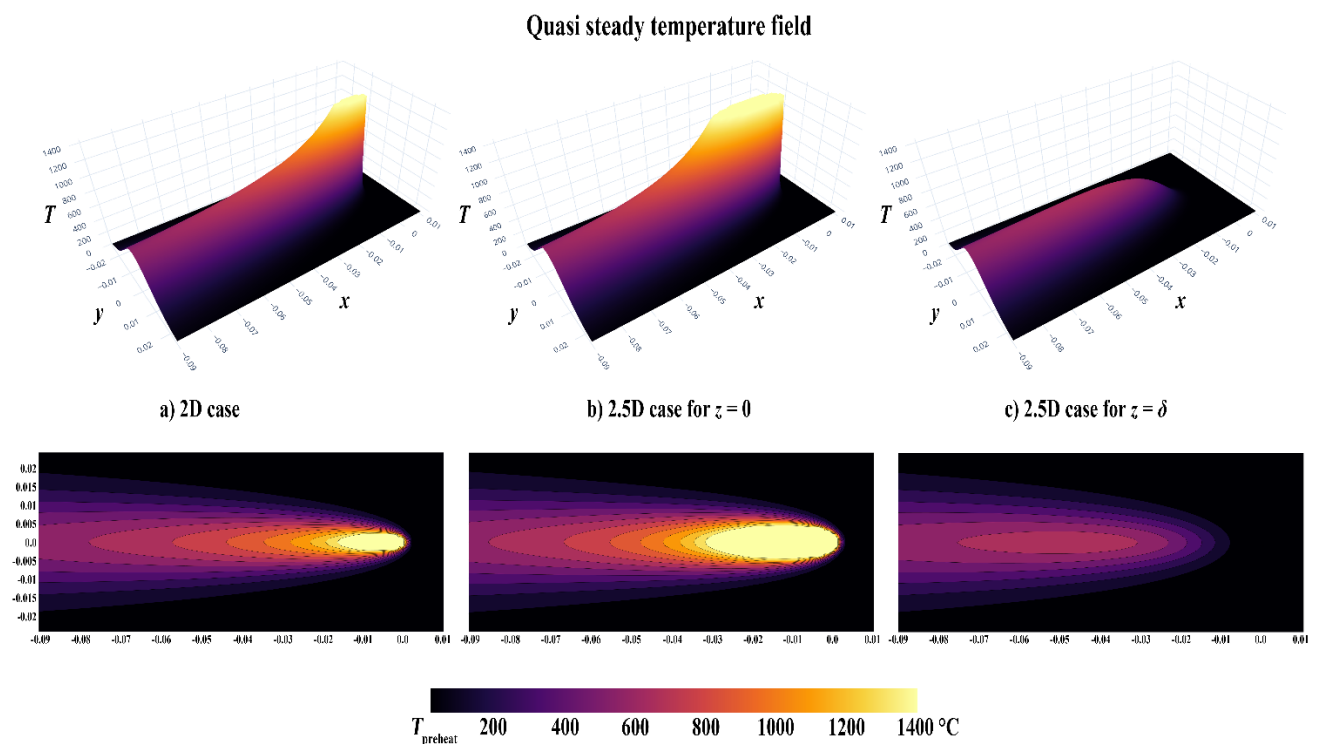


Figure 7. Two-dimensional and Two and half-dimensional temperature fields around moving heat source – results of the calculation according to equations (1), (2) and (3)

The idea of this work is to check the measured temperatures at the 40th second of the welding process in the point with coordinates: $x = 17.6 \text{ mm}$; $y = 2.65 \text{ mm}$. As it can be seen from Figure 6,

the measured value of the temperature in the point (0.0) is 589.04 °C, so we should first find the distance from the heat source where it gets the measured value of 589.04 °C.

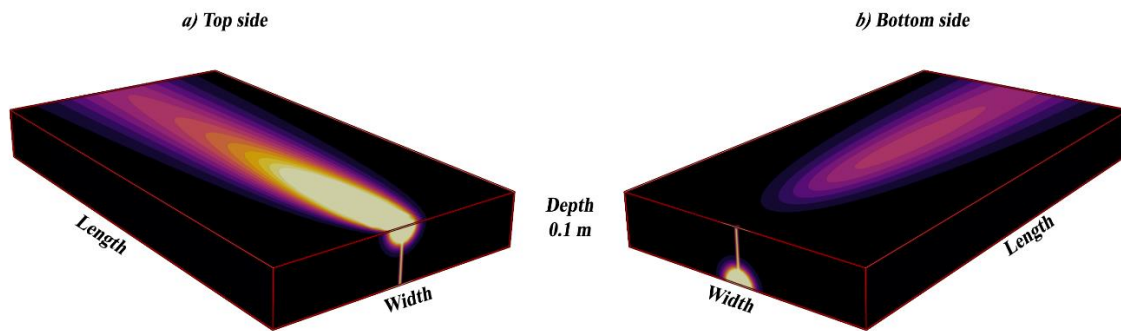


Figure 8. Three-dimensional representation of the temperature field from the top and bottom side of the 2.5D model

If the values of thermal and technological properties are incorporated in Equation (1), (2) and (3), then the calculation results can be shown as it is done in Figure 7, Figure 8 and Figure 9. Two and Two and half-dimensional temperature field represented by areas of different colors between isotherms are shown in Figure 7 and Figure 8. In Figure 9, thick lines represent the cases of adiabatic heating of the plate, while dashed lines represent the cases with heat transfer to the environment by radiation and convection.

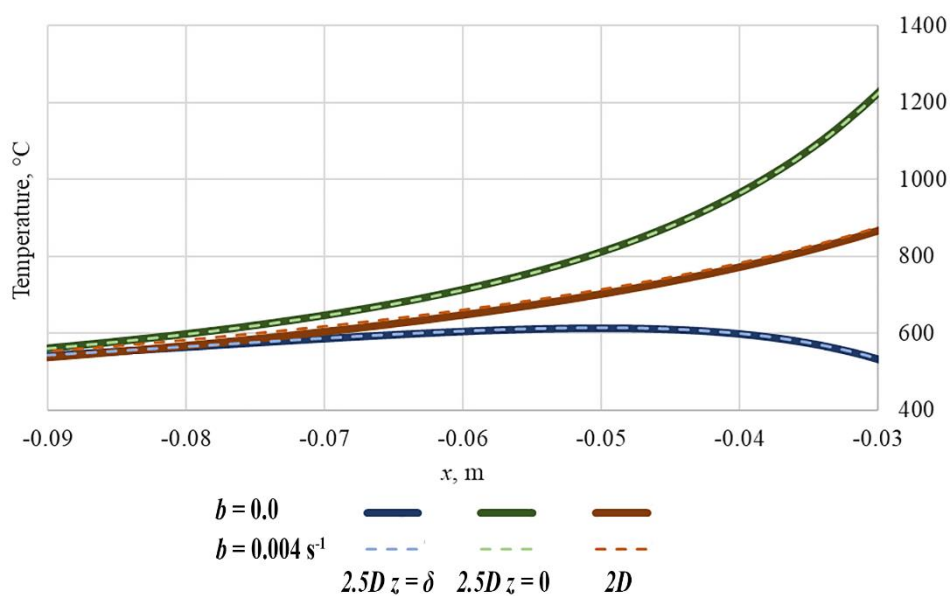


Figure 9. Temperature as a function of x at $y = 0.00265$, thick line, $b = 0.0$; dashed line, $b = 0.004 \text{ s}^{-1}$

It can be read from calculated temperature fields that the temperature distances differed for different models. The measured distance between the three temperatures of 589.036, 541.961 and 477.271 °C in the thermogram are 17.6 mm and 19.2. mm respectively. The 2D model gives distances of 16.2 and 14.8 mm, while the 2.5D models for $z = 0$ and $z = \delta$ give distances of (12.6 mm, 23.2 mm) and (13.7 mm, 6.2 mm) respectively. As already mentioned, deviations were expected, both because of the imperfection of the model and because of error in the temperature readings from the thermogram. It can be seen that temperature significantly depends on the value x , in a way that, behind the heat source ($x < 0$) it decreases with the distance from the heat source; at the heat source it reaches maximum (tends to infinity), and in front of the heat source, ($x > 0$) it falls abruptly. The decrease of the temperature gradient in front of the heat source is very large, while it is not large behind the heat source. Figure 10 shows the temperature function of the y coordinate, at various values of x , while Figure 11 shows the symmetry characteristic of the welding process with respect to x -axis.

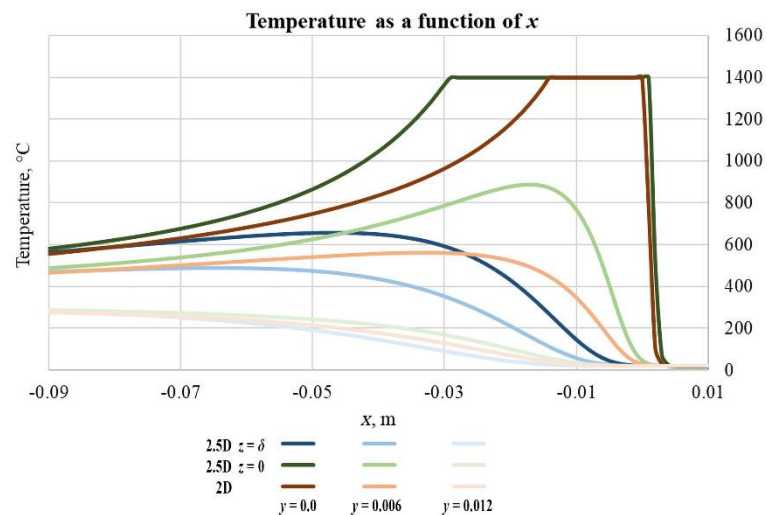


Figure 10. Temperature as a function of x at $y = 0.0, 0.006$ and 0.0012 m

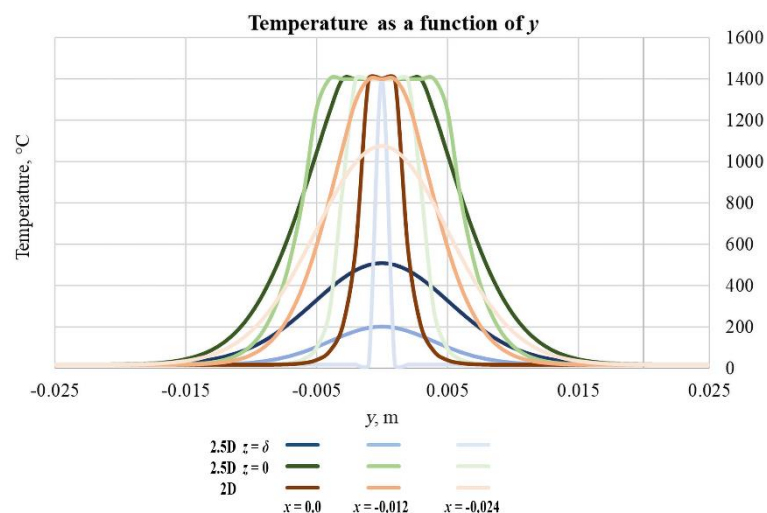


Figure 11. Temperature as a function of y at $x = 0.0, -0.012$ and -0.0024 m

5 CONCLUSION

The brief mathematical analysis of the temperature field at one point has shown that this mathematical model is very sensitive to the coordinates of the points, especially at a longer distance from the heat source. In this case the exponential function shows particularly high values, while Bessel function shows very small values. A similar conclusion can be drawn for results from thermogSBWram, even a small deviation in measured coordinates can contribute to different results because of stochastic properties of temperature. Therefore, it's necessary to do averaging of the temperature values for the observed area if we want to be able to compare the model more accurately with the experiment. The 2.5D model is greatly influenced by the velocity value of the considered source and for some cases the deviation in results could be too great, giving invalid results. In our case, the velocity of the heat source is great and in such case of fast-moving heat source, the results are at the limits of validity and better models should be considered. Both analytical models give promising results for slow moving sources, and it is up to the user to evaluate which one to apply, keeping in mind the human error while reading the results. We can conclude that infrared thermography is practical weld-monitoring option able to provide a reliable estimation, but some methods like using isotherms or averaging of temperatures during reading the results from thermogram are needed to get the reliable results.

6 REFERENCES

- [1] Mahrle, A.; Schmidt, J.; Weiß, D.: Simulation of Temperature Fields in Arc and Beam Welding. *Heat and Mass Transfer* 36 (2000), 165-171.
- [2] Rosenthal, D.: The theory of moving sources of heat and its application to metal treatment, *Trans. ASME* 68 (1946) 849–865.
- [3] Rykalin, R.R.: Calculation of Heat Processes in Welding, Educational Lecture, Am. Weld. Soc. Annual Assembly, New York, 1961.
- [4] Wang, S.; Goldak, J.; Zhou, J.; Tchernov, S.; Downey, D.: Simulation on the thermal cycle of a welding process by space–time convection–diffusion finite element analysis, *International Journal of Thermal Sciences* 48 (2009), 936–947.
- [5] Van Elsen, M.; Baelmans, M.; Mercelis, P.; Kruth, J.-P.: Solutions for modelling moving heat sources in a semi-infinite medium and applications to laser material processing, *International Journal of Heat and Mass Transfer* 50 (2007) 4872–4882.